

Supplemental information - Rheological implications of embedded active matter in colloidal gels

Interaction potential for colloidal particles

The interaction potential for a colloidal particles in our experiments as a function of the separation distance, r , is given by a sum of the van der Waals attraction, $V_{vdw}(r)$, and screened electrostatic repulsion, $V_{charge}(r)$:

$$V(r) = V_{vdw}(r) + V_{charge}(r)$$

The van der Waals attraction is given by:

$$V_{vdw}(r) = -\frac{A}{6} \left\{ \frac{2R^2}{(4R+r)r} + \frac{2R^2}{(2R+r)^2} + \ln\left(\frac{r}{4R+r}\right) \right\}$$

where A is the Hamaker constant (1.4×10^{-20} J for polystyrene in water) and R is the particle radius ($R = 0.5 \mu\text{m}$)¹. The electrostatic repulsion is given by:

$$v_{charge}(r) = \frac{Z}{\kappa^2} \exp(-\kappa R)$$

where κ^{-1} is the Debye length ($\kappa^{-1} = 0.695$ nm for $[\text{MgCl}_2] = 64$ mM) and Z is the interaction constant ($Z = 176 \text{ J m}^{-2}$).

Supplemental Figures

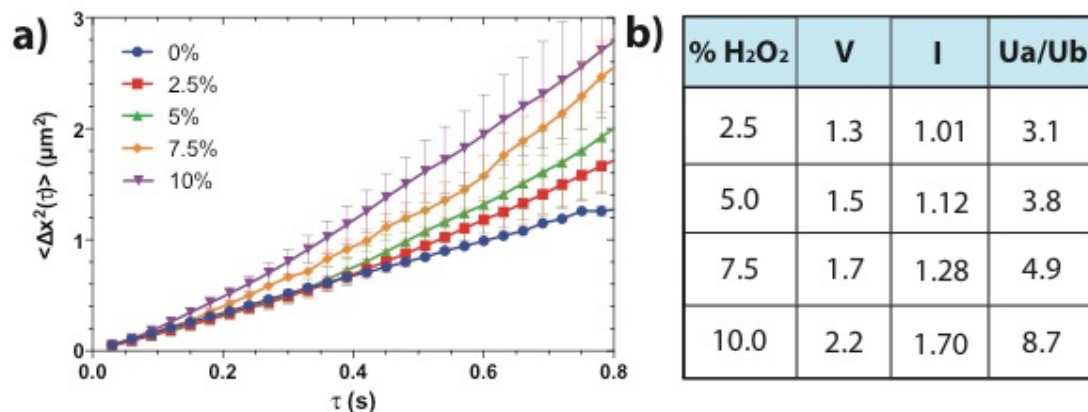


Figure S1. Microdynamics and energy of free active colloids. a) Mean squared displacement of free active Janus colloids at each hydrogen peroxide concentration. b) Velocity (V), run length (l), and active energy (Ua/Ub) at each hydrogen peroxide concentration. Velocity is shown in units $\mu\text{m/s}$ and run length is shown in μm . Calculations are performed as per the method described in ref [1]². The velocities were calculated by fitting short time mean squared displacement at each H_2O_2 concentration to expressions developed by Howse et. al.³. Free particle velocities were converted to active energies following the concept of the swim pressure developed by Takatori et. al.⁴.

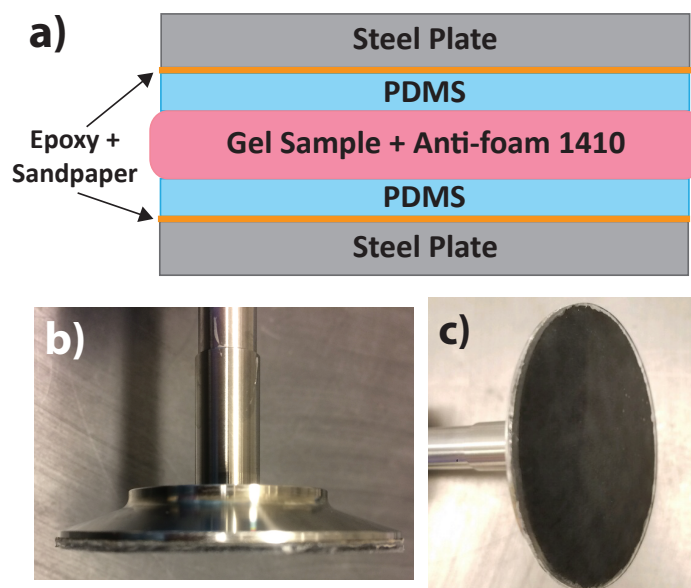


Figure S2. Design and production of PDMS plates for active gel rheology experiments. a) Schematic of PDMS plate attached to steel fixture using epoxy and sandpaper with adhesive backing. PDMS is attached to sandpaper with adhesive back using Devcon 5

minute epoxy. Photographs of PDMS attached to 50 mm stainless steel fixture shown in b) and c).

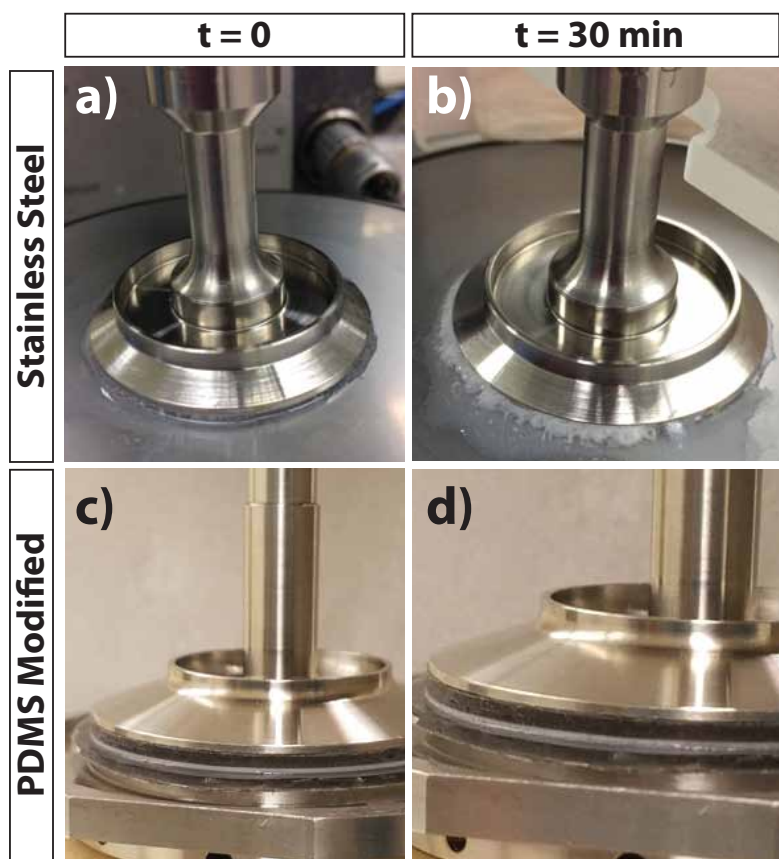


Figure S3. a) At time $t = 0$, there are no apparent O_2 bubbles formed under the stainless steel fixture. b) After 30 minutes, O_2 bubbles formed from H_2O_2 decomposition nucleate and grow when active gels are confined in a stainless steel fixture. With PDMS modified stainless steel fixtures, shown in c) and d), O_2 can diffuse into PDMS film, which helps prevent the formation of O_2 bubbles.

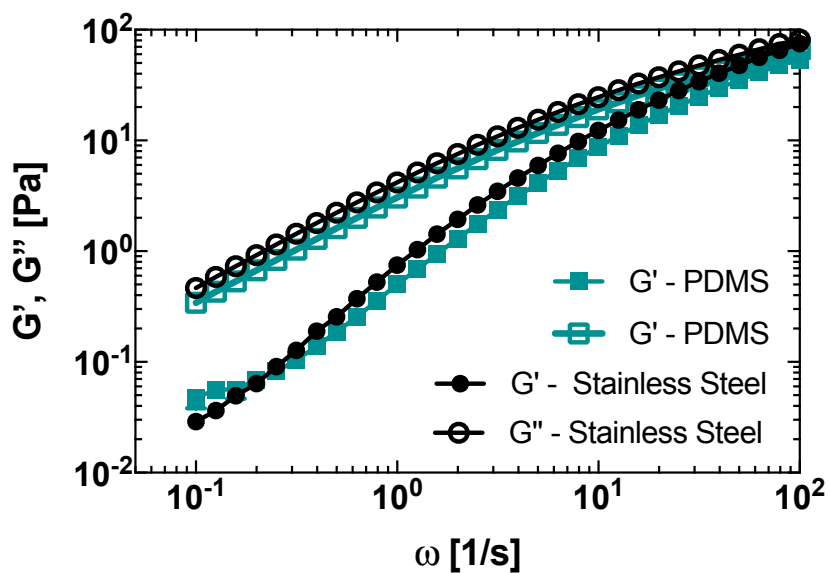


Figure S4. Accuracy of PDMS modified rheometer fixtures. Frequency dependent linear viscoelastic moduli were measured for with 4.0 wt. % aqueous solution of PEO (MW = 10^6) with stainless steel fixtures and fixtures modified with PDMS Sylgard 182.

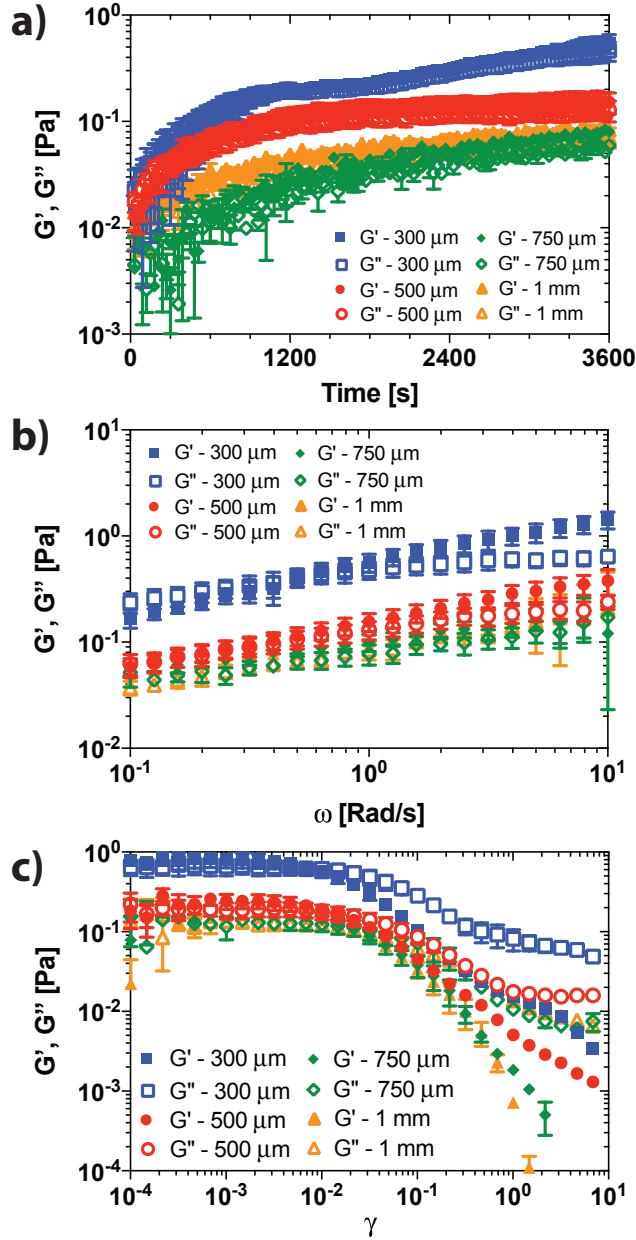


Figure S5. Gap study with 50 mm steel plate. a) Transient behavior of the linear viscoelastic moduli were monitored at a $\omega = 1 \text{ s}^{-1}$ and $\gamma = 0.003$. b) Frequency sweep was performed at $\gamma = 0.003$. c) Strain sweep was done at $\omega = 1 \text{ s}^{-1}$.

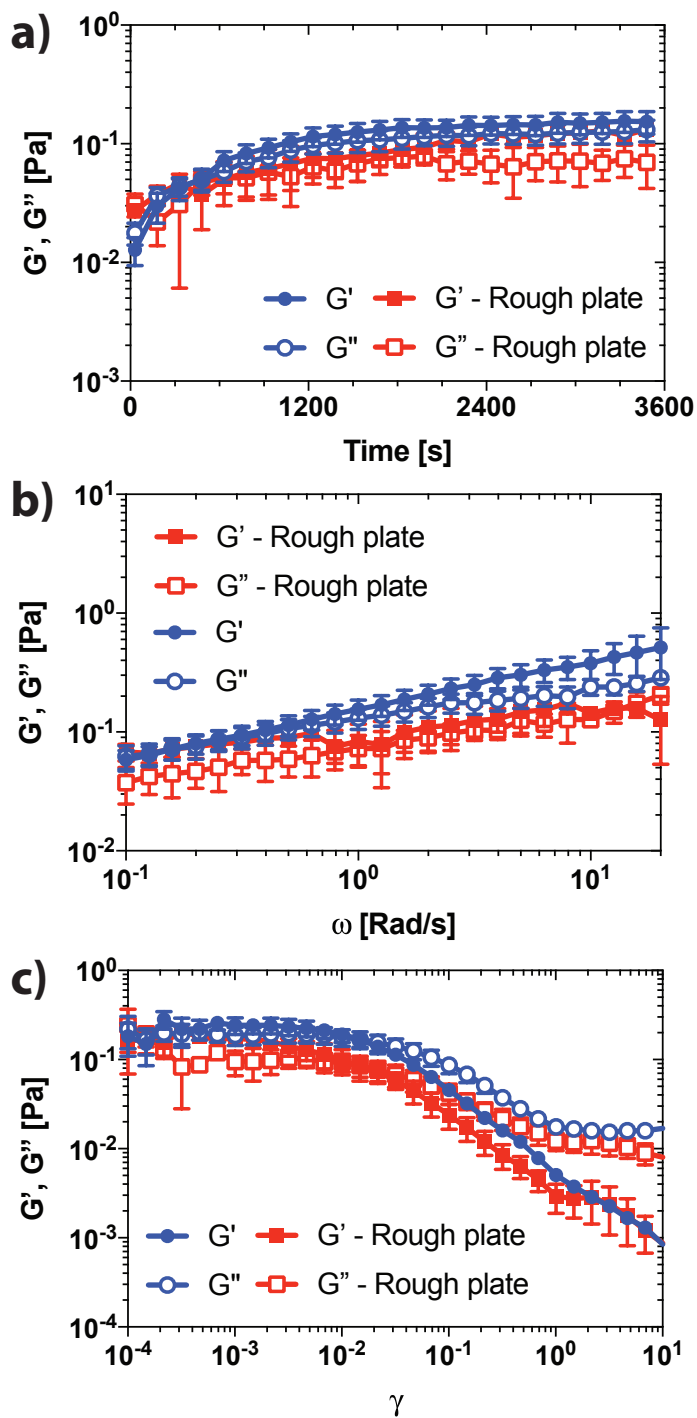


Figure S6. Comparison of rheology characterized with a smooth stainless steel plate and with a sandblasted steel plate for passive gels. a) Transient linear viscoelasticity at $\omega = 1 \text{ s}^{-1}$ and $\gamma = 0.003$. b) Frequency dependent linear viscoelasticity moduli ($\gamma = 0.003$). c) Strain sweep at $\omega = 1 \text{ s}^{-1}$.

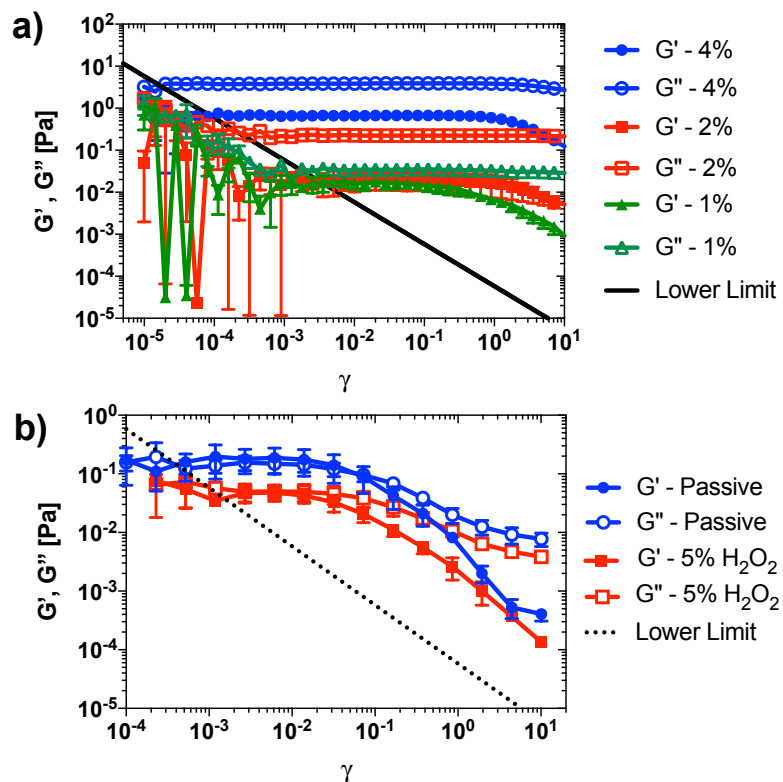


Figure S7. Determining lower stress limit of measurements through a) oscillatory strain sweeps of aqueous PEO solutions (MW = 10^6) prepared at 1 wt. %, 2 wt.%, and 4 wt.%. Solid line indicates lower stress limit. Solid line shows lowest resolvable modulus calculated from lower torque limit of the rheometer. b) Oscillatory strain sweeps of passive and active gels are above the lowest resolvable modulus across all strain amplitudes larger than 10^{-3} .

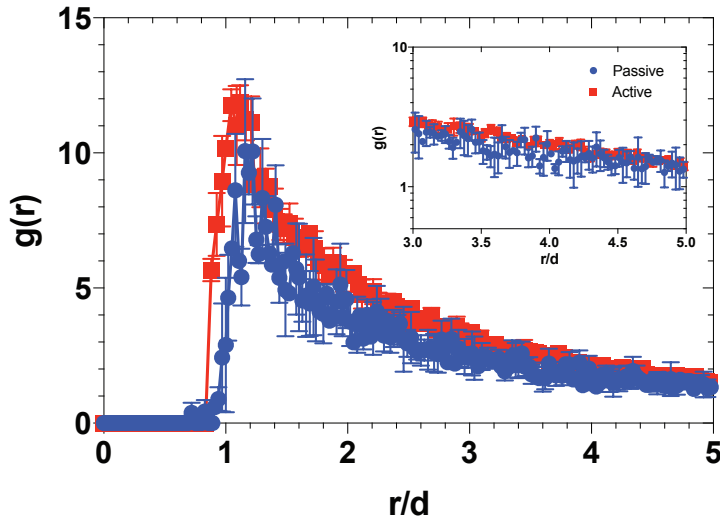


Figure S8. Radial distribution function, $g(r)$, of passive and active gels. The fractal dimension, d_f , and average cluster size, R_c , were calculated from $g(r)$ for passive and active gels. The fractal dimension was calculated by fitting the slope of $g(r)$, shown in the inset, following methods described by Lattuada et. al⁵. The fractal dimension was calculated using expressions described by Krall and Weitz⁶.

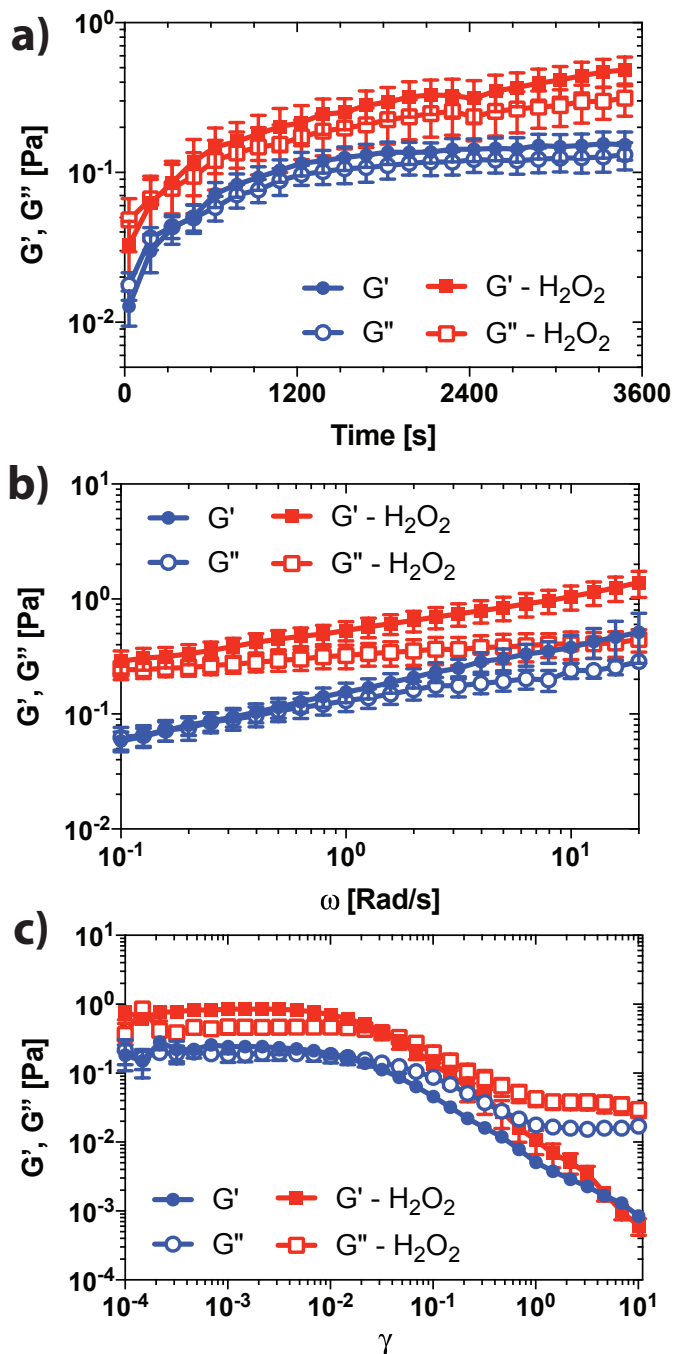


Figure S9. Comparison of rheology of passive gels with and without hydrogen peroxide measured with a 50 mm steel plate at a gap of 0.5 mm at 20°C. a) Transient rheology at $\omega = 1 \text{ rad/s}$ and $\gamma = 0.003$. b) Frequency dependent viscoelastic moduli at $\gamma = 0.003$. c) Strain sweep at $\omega = 1 \text{ rad/s}$. The elastic moduli of the gels stiffens by about 40% after addition of hydrogen peroxide.

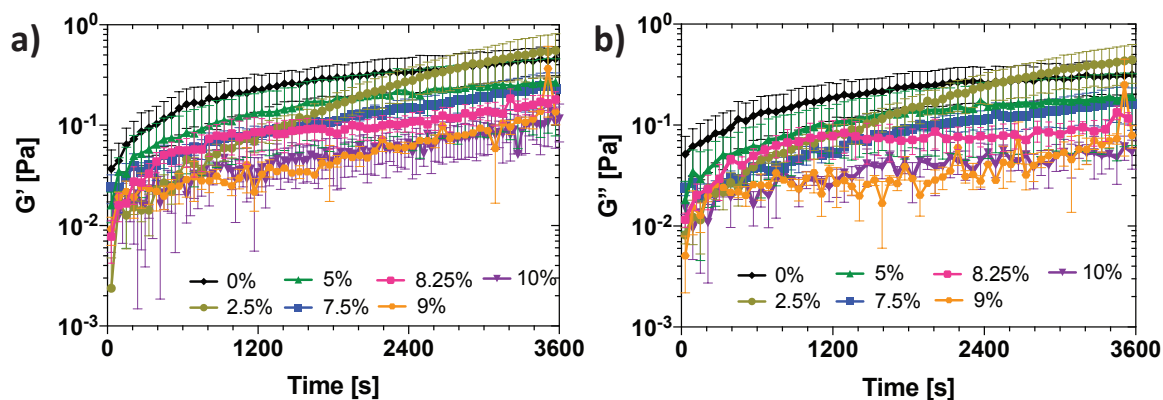


Figure S10. Viscoelastic moduli of active gels as a function of time at each of the hydrogen peroxide concentrations studied.

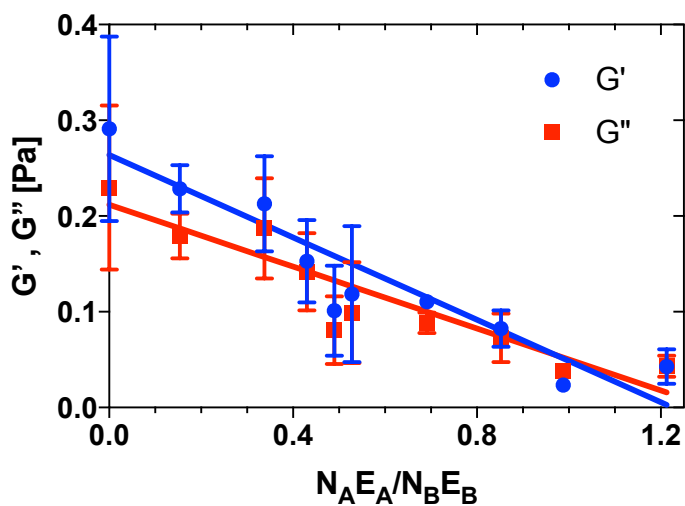


Figure S11. Viscoelastic moduli as a function of the scaled active energy input to the system ($\gamma = 0.003$, $\omega = 1 \text{ s}^{-1}$, $t = 1800 \text{ s}$).

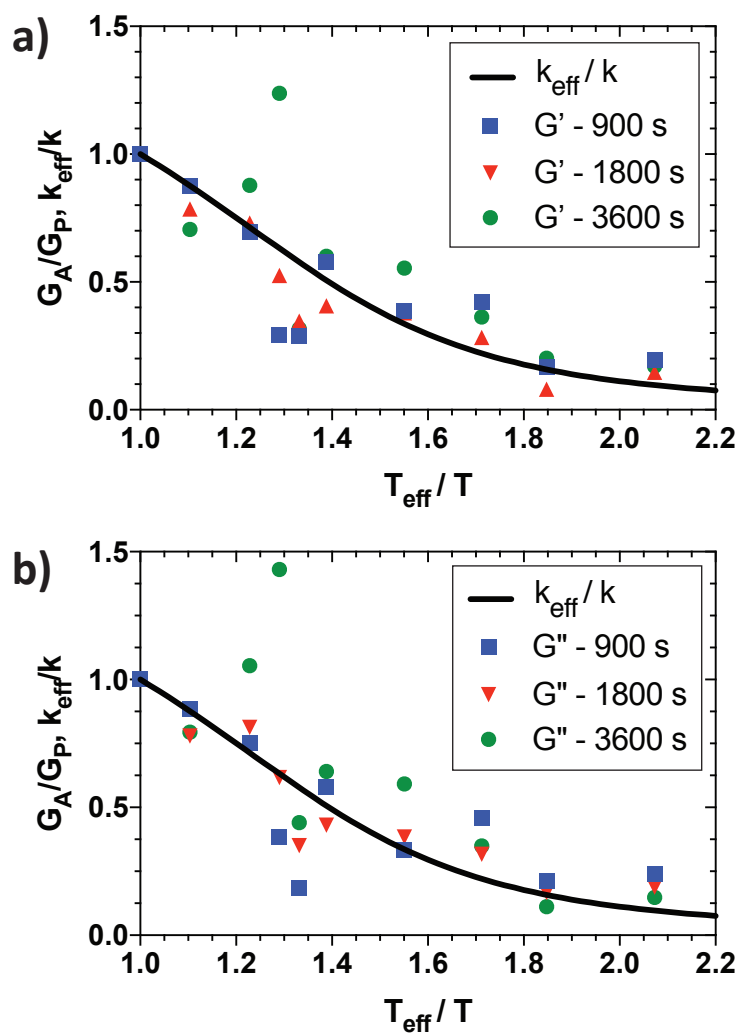


Figure S12. Time dependent comparison of experimentally measured a) elastic and b) viscous modulus with calculated effective spring constant.

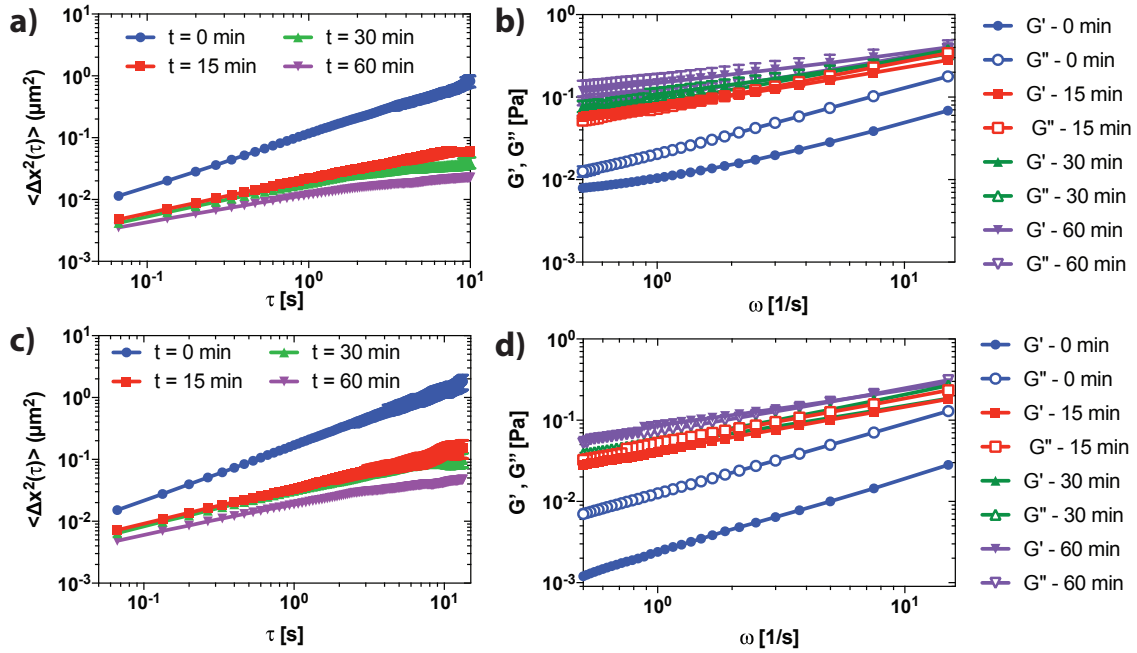


Figure S13. Microdynamics and microrheology of passive and active gels. Mean squared displacement of a) passive and c) active gels at $t = 0, 15, 30$, and 60 minutes after addition of salt to induce gelation. Microdynamic measurements are converted to frequency dependent viscoelastic moduli for b) passive and d) active gels using the generalized Stokes-Einstein equation.

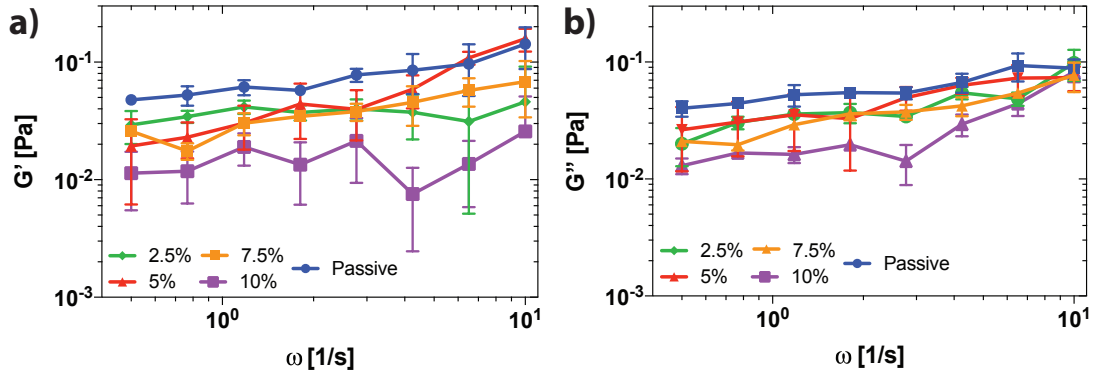


Figure S14. Frequency dependence of a) G' and b) G'' for passive and active gels. Active gels have a fixed ratio of active to passive colloids and 2.5% , 5.0% , 7.5% or 10% H_2O_2 ($\gamma = 0.003$, $t = 900$ s).

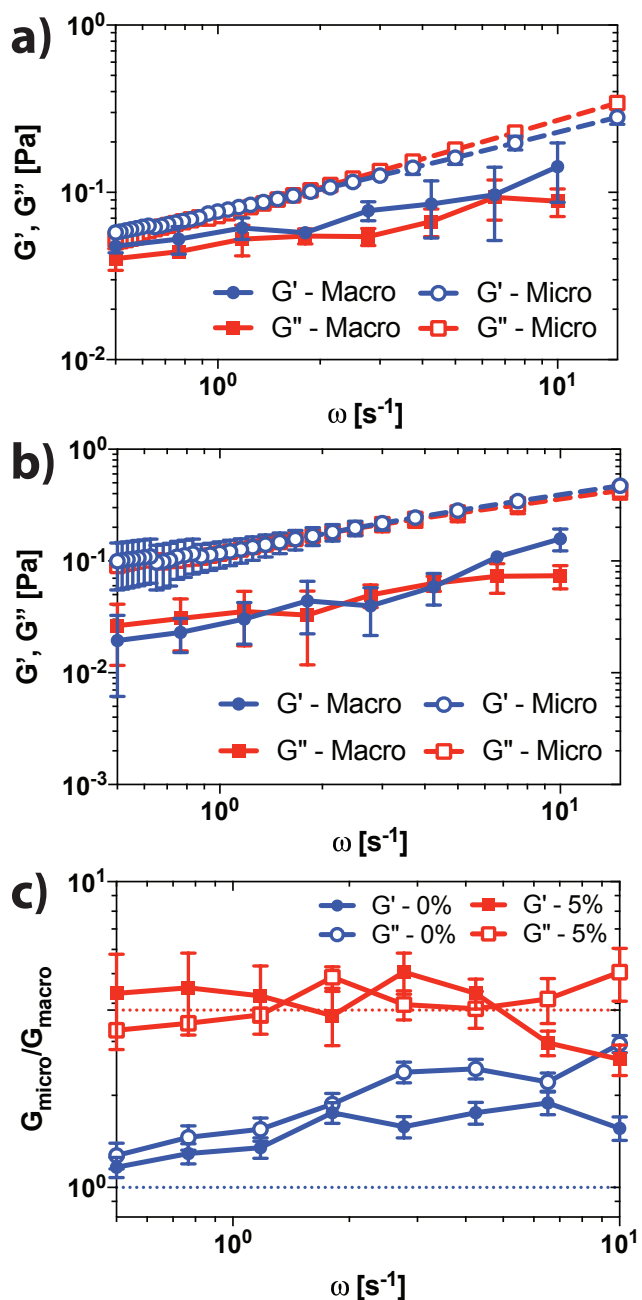


Figure S15. Comparing frequency dependent G' and G'' obtained from microrheology and mechanical rheology for a) passive gels and b) active gels with 5% H_2O_2 . These data were collected 15 minutes after addition of salt to allow sufficient time for particle gelation. c) The ratio of G' and G'' obtained from microrheology and mechanical rheology as a function of frequency. The moduli obtained from microrheology are higher than the mechanical rheology values for both a) passive and b) active gels with 5% H_2O_2 ($E_a/E_p = 3.8$). The difference between microrheology and mechanical rheology of the passive gels is greatest at high frequencies; it is as a factor of 2.0 for G' and 3.0 for G'' . The amount of overprediction by microrheology is larger for active gels, up to a factor of 5.0 for G' and G'' .

References

1. Israelachvili, J. N. *Intermolecular and Surface Forces*. (Elsevier Inc., 2011).
2. Szakasits, M. E., Zhang, W. & Solomon, M. J. Dynamics of Fractal Cluster Gels with Embedded Active Colloids. *Phys. Rev. Lett.* **119**, (2017).
3. Howse, J. R. *et al.* Self-Motile Colloidal Particles : From Directed Propulsion to Random Walk. *Phys. Rev. Lett.* **99**, 048102 (2007).
4. Takatori, S. C., Yan, W. & Brady, J. F. Swim pressure: Stress generation in active matter. *Phys. Rev. Lett.* **113**, 028103 (2014).
5. Lattuada, M., Wu, H., Hasmy, A. & Morbidelli, M. Estimation of fractal dimension in colloidal gels. *Langmuir* **19**, 6312–6316 (2003).
6. Krall, A. H. & Weitz, D. A. Internal Dynamics and Elasticity of Fractal Colloidal Gels. *Phys. Rev. Lett.* **80**, 778–781 (1998).